1997 Elsevier Science B.V.
Hydrotreatment and hydrocracking of oil fractions
G.F. Froment, B. Delmon and P. Grange, editors

Novel Hydrotreating Catalysts Based on Synthetic Clay Minerals

R.G. Leliveld, W.C.A. Huyben, A.J. van Dillen, J.W. Geus and D.C. Koningsberger

Department of Inorganic Chemistry, Debye Institute, University of Utrecht,
P.O. Box 80083, 3508 TB Utrecht, The Netherlands

Saponites with Co, Ni, Zn, Mg and combinations of Co and Mg in the octahedral layer were synthesised. Their applicability as catalysts and supports for hydrotreating catalysts was investigated. The stability of these clays in a sulfidic environment was studied using Temperature Programmed Sulfidation. The catalytic performance of the saponites both bare and impregnated with Co/Mo was tested in the hydrodesulfurisation of thiophene.

1. Introduction

In modern refineries hydrocracking of heavy oil feedstocks to high-value transportation fuels is a flexible process dependent on feed and desired product selectivity. Most catalysts currently used are bifunctional consisting of a hydrogenating component, such as noble metals or transition metal sulfides, together with an acidic function usually incorporated in the support [1-2].

One of the first hydrocracking catalysts to be commercially used was a supported Fe montmorillonite catalyst developed by ICI in the late 1930's [3]. Nowadays almost all hydrocracking catalysts are based upon zeolites due to their favorable acidic and textural properties [4]. However, the zeolite structure can lead to pore exclusion of the large molecules present in heavy crudes. The limited size of zeolite pores has led to a renewed interest in acidic clay minerals as an alternative support since the platelike structure of clays might avoid transport limitations [5-6]. Clays belong to the group of phyllosilicates: layered or two-dimensional silicates build of octahedral and tetrahedral sheets as represented in Figure 1.

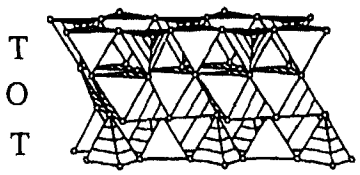

Figure 1. Structure smectite H_x-$Mg_3Si_{4-x}Al_xO_{10}(OH)_2$: *T, tetrahedral and O, octahedral sheet*

The varying and difficult to control texture and composition of natural clays and the presence of impurities are severe drawbacks to the use as catalysts [7-9]. Recently, our group reported on a novel route to synthesize a class of 2:1 trioctahedral clays called saponites [10] at

nonhydrothermal conditions. In saponites tetrahedral Si atoms are partly substituted by Al atoms, while the octahedral layer contains divalent cations. The new synthesis route allows careful control of the clay's texture and acidity.

This study is directed towards the aptness of synthetic saponites with differing octahedral ions as catalysts and as support for hydrocracking catalysts with emphasis on their resistance against sulfur. For this reason, saponites with Co, Ni, Zn, Mg and combinations of Co and Mg incorporated in the octahedral sheet were synthesised and studied with Temperature Programmed Sulfidation and XRD/TEM. The catalytic activity of the bare saponites and of Co/Mo impregnated samples were tested in the hydrodesulfurisation of thiophene. A good hydrocracking catalysts requires a well dispersed hydrogenating function to prevent excess cracking on the acidic sites. The performance in Thiophene hydrodesulfurisation (HDS) can offer insight in the dispersion of the metal sulfides on the surface of the clay support [11].

2. Experimental

Catalyst preparation

Saponites with Mg, Zn, Co and Ni as octahedral ions and mixtures of Mg and Co were synthesised at 363 K and 1 atmosphere from a Si/Al gel (Si/Al ratio 12.3) and a solution containing urea and the M^{2+}-nitrate [10]. After ion-exchange with ammonium (1M NH_4Cl solution) the saponites were dried at 393 K and calcined at 723 K. The samples are denoted by the octahedral ions followed by their mutual ratio e.g. Co:Mg 1:11 saponite. Mo and Co impregnated catalysts were prepared by incipient wetness impregnation of the saponite supports with aqueous solutions containing the required amounts of $(NH_4)_6Mo_7O_{24}\cdot 6\ H_2O$ and $Co(NO_3)_3\cdot 6\ H_2O$. The impregnated saponites were subsequently dried in an air flow at 298 K, dried in stagnant air at 393 K and calcined at 723 K.

Characterisation

Catalyst samples were examined with X-ray powder Diffraction (XRD) with an Enraf Nonius FR590 diffractometer using CoKα radiation. Transmission Electron Microscopy (TEM) was performed with a Philips EM-420 instrument operated at an accelerating voltage of 120 kV. Diffuse Reflectance Infrared Fourier Transform (DRIFT) spectra were recorded on diluted samples (10% in KBr) using a Perkin Elmer 1600 series spectrometer. Extended X-ray Absorption Fine Structure (EXAFS) measurements were performed at EXAFS station 9.2 of the SRS at Daresbury (U.K.). The saponite samples were pressed into self-supporting wafers and mounted in an in-situ EXAFS cell [12]. The spectra were recorded for the Co-K edge at liquid nitrogen temperature. Details of the data analysis have been described elsewhere [13-14]. Phase shifts and backscattering amplitudes from reference compounds were used to calculate the EXAFS contributions: CoO for the Co-Co and $Co(OH)_2$ for the Co-O scatterer-backscatterer pair. The Co-Mg and Co-Si references were theoretically calculated with the FEFF-3.1 code [15].

Temperature-Programmed Sulfidation and Hydrodesulfurisation of Thiophene

Temperature Programmed Sulfidation profiles were recorded in an automated microflow apparatus. The samples (1.0 ml, sieve fraction 150-425 μm) were sulfided in a 100 ml/min flow of $H_2S/H_2/Ar$ (10/40/50). After 30 min at room temperature the temperature was linearly raised (5K/min) to 673 K. The H_2S concentration before and after the reactor was monitored with a Varian UV/Vis spectrophotometer at λ=232 nm. After 30 min at 673 K the flow was

switched to 51.2 ml/min thiophene/H_2/Ar (2.4/87.9/9.6). Analysis of the reactor effluent was done with a gaschromatograph using a Chrompack CP-sil-5 CB column and FID. The catalytic activity in the conversion of thiophene was measured at temperatures between 673 and 423 K after 6 hr on stream at 673 K (atmospheric pressure).

3. Results

3.1 Characterization

After synthesis for 20 hours and calcination at 723 K all saponites were characterised with XRD, TEM and nitrogen physisorption. XRD confirmed that in all cases a 2:1 clay triooctahedral clay was formed as indicated by the presence of the characteristic d(060) reflection at about 1.54 Å [16]. TEM showed the saponites to consist of small platelets with an open 'house of cards' structure, as shown in Figure 2a for a Co saponite. The size of the platelets varied from 300 nm for the Zn-saponite to 25-40 nm for the Mg, Ni and Co-clays. The B.E.T. surface areas reflected the size of the platelets varying from 105 m^2/g (0.14 ml/g) for the Zn-saponite to 570 m^2/g (0.46 ml/g) for the Mg sample. The surface areas of the mixed Co-Mg saponites were intermediate between the pure Mg and Co saponite (410 m^2/g).

The structure of the mixed Co-Mg saponite platelets was quite uniform as revealed by TEM. There was no indication of separate Co and Mg platelets, as EDX confirmed the presence of both Co and Mg within the same clay platelet.To study the distribution of the Co and Mg cations within the octahedral layer the samples were characterised with DRIFT and EXAFS.

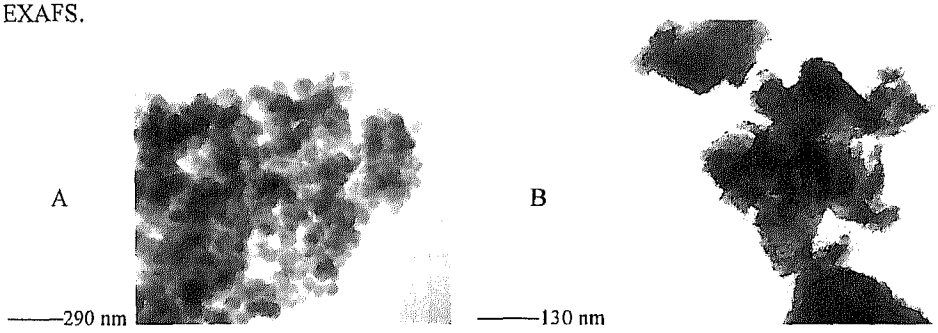

Figure 2. TEM photograph of a fresh (a) and sulfided (b) Co-saponite Si/Al=12.3

DRIFT and EXAFS

The hydroxyl stretching range between 3800 and 3100 cm^{-1} of the pure and mixed Co-Mg saponites is represented in Figure 2. All spectra were recorded at 673 K under an Ar flow to minimise the amount of water present within the saponite samples. The spectra contained two bands referred to as ν_1(OH) and ν_2(OH). The position of the ν_2(OH) band at 3723 cm^{-1} was independent of the Co-Mg ratio except for the pure Co saponite. The broad ν_1(OH) band varied from 3762 to 3615 cm^{-1} for the Mg and Co saponite, respectively.

The Co saponite and Co-Mg saponites with Co:Mg=1:29 and 1:1 were characterised with EXAFS of the Co-K edge. The absolute part of the k^3 weighed Fourier Transform of the three samples,as shown in Figure 3, exhibited two shells. The first shell between 1 and 2 Å (phase

uncorrected) is due to the nearest six oxygen neighbours of the Co ions in the octahedral layer. The second shell between 2.2 and 3.4 Å is made up from neighbouring octahedral cations and the Si/Al atoms of the tetrahedral sheet. When the amount of Mg in the octahedral layer increased the amplitude of the second shell drasticly reduced. This reduction is due to a destructive interference of the Co-Co and Co-Mg scatterer-backscatter contributions [17]. The results of the data analysis results are presented in Table 1.

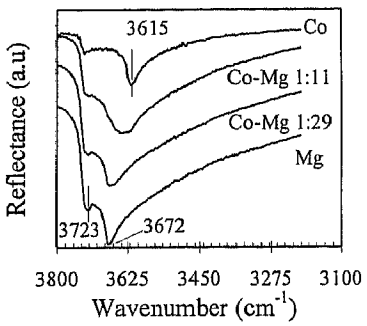

Figure 3: DRIFT spectra of Co-Mg saponites

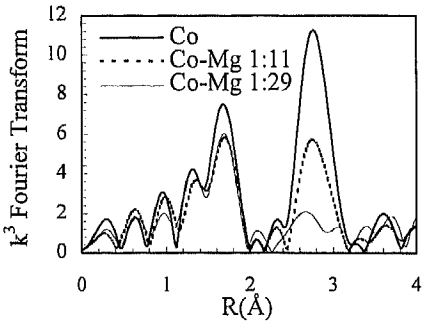

Figure 4. k^3 weighted Fourier Transform

The number of neighbours and the interatomic distances for pure Co-saponite were in accordance with the known crystal structure [17]. As Si and Al are neighbours in the periodic table the backscattering phase and amplitude are similar justifying a fit of the k^3 weighted Fourier Transform with 4 Si neighbours at 3.27 Å. The fit of the Co-Mg samples incorporated the expected Mg neighbours at a slightly shorter distance than the Co ions.

Table 1
Data Analysis Results Co-K EXAFS of Co-Mg saponites, R-space fit, k^3 Fourier Transform

scatterer	N	$\Delta\sigma^2$ (10^{-4} Å^2)	R (Å)	ΔE_0 (eV)[1]
Co-saponite				
O	6.1	-3	2.09	-0.4
Co	6.2	2	3.11	1.4
Si	4.1	33	3.27	5.3
Co-Mg 1:1 saponite				
O	6.0	-7	2.08	0.4
Mg	2.5	104	3.02	1.0
Co	2.5	168	3.14	1.5
Si	4.1	-2	3.27	2.6
Co-Mg 1:29 saponite				
O	6.0	17	2.05	2.3
Mg	5.8	6	3.12	1.5
Co	0.4	33	3.15	2.3
Si	4.5	-13	3.23	8.8

[1] The estimated accuracy of the fit parameters is 20 % for N and $\Delta\sigma^2$ and 1% for R and ΔE_0

3.2 Temperature Programmed Sulfidation

Figure 5 shows the H_2S absorption per unit weight for the pure Mg, Zn, Co and Ni saponites.

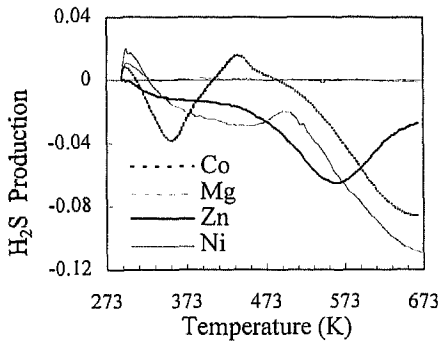

Figure 5. TPS of Co, Ni, Zn and Mg saponite

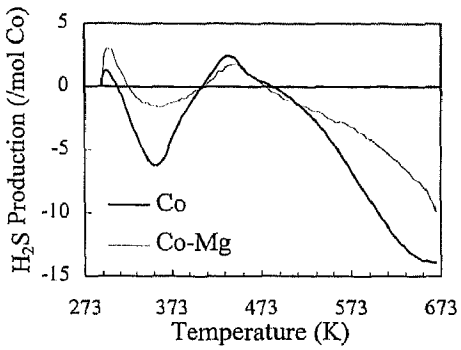

Figure 6. TPS of Co and Co-Mg 1:1 saponite

Except for Zn, all saponites showed a desorption of H_2S between 298 and 343 K due to release of physisorbed H_2S. When the temperature was raised both the Co, Ni and Zn saponites consumed a large amount of H_2S. The consumption of H_2S was not completed at 673 K. When the H_2S absorption was monitored isothermally at 673 K, the consumption quickly decreased. Only when the temperature was further raised above 673 K an extra H_2S uptake was observed, indicating the extent of sulfidation to be predominantly temperature controlled. The Mg-saponite does not show any uptake or release of H_2S at temperatures higher than 353 K pointing to a stable oxidic structure. Figure 6 presents the TPS profiles of the Co and Co-Mg 1:1 saponite. The H_2S uptake per Co atom for the mixed Co-Mg saponite was substantially less than for the Co-saponite. This points to a stabilisation of the Co atoms in the clay lattice of the Co-Mg saponites relative to the pure Co saponite.

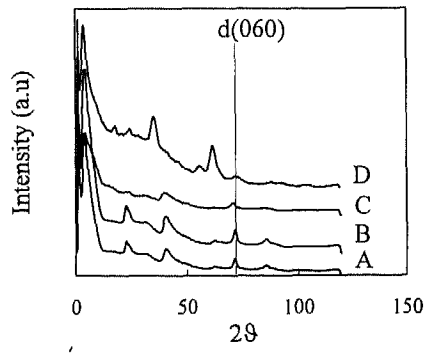

Figure 7. XRD of fresh and sulfided Mg (A and B) and Co saponite (C and D)

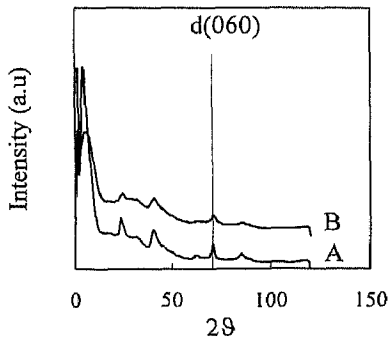

Figure 8. XRD of fresh (A) and sulfided (B) Co-Mg 1:1 saponite

The XRD spectra of a fresh Mg and Co saponite and those after sulfidation are shown in Figure 7. The XRD pattern of the Mg-saponite after sulfidation did not change with respect to the fresh saponite whereas for Co it was quite different. The characteristic clay reflections at 1.54 Å (71° 2θ) and 2.63 Å (40° 2θ) practically disappeared and two reflections at 1.74 Å (62° 2θ) and 2.96 Å (35° 2θ) characteristic of Co_9S_8 evolved. In agreement with the TPS results, XRD patterns of sulfided Ni and Zn saponites similarly showed the presence of crystalline Ni_3S_2 and β-ZnS, respectively, and a loss of the clay structure. Figure 1b contains the TEM photograph of the sulfided Co-saponite. The small clay platelets disappeared and instead large crystalline particles were formed together with amorphous silica-alumina. In contrast, XRD spectra of the fresh and sulfided Co-Mg 1:1 saponite are shown in Figure 8. After sulfidation the 2:1 clay structure was still present as indicated by the d(060) reflection and confirmed by TEM. The sample suffered some loss of crystallinity as indicated by the broadening of the clay reflections leading to a decrease in intensity.

3.3 Thiophene Hydrodesulfurisation

The thiophene conversion of the bare Co,Ni, Zn and Mg saponites and those impregnated with 7.5 wt% MoO_3 is presented in Figure 9a and 9b, respectively. The usual reaction products were observed, viz., 1-butene, cis- and trans-butene, butane and H_2S. Additionally the Co and Ni-catalysts produced substantial amounts of iso-butane (up to 8 %). As shown in Figure 9a Zn and Mg saponites did not exhibit any HDS activity. The Ni and Co-saponite, however, were quite active with conversions of 77 and 42 %, respectively. When Mo was impregnated the Mg-saponite became active exhibiting a conversion of 21 % at 673 K. Addition of Mo to the Co-saponite lowered the activity from 42% to 20%. The performance of the Ni-saponite remained more or less unchanged when promoted with Mo (conversions of 77 vs.82 %).

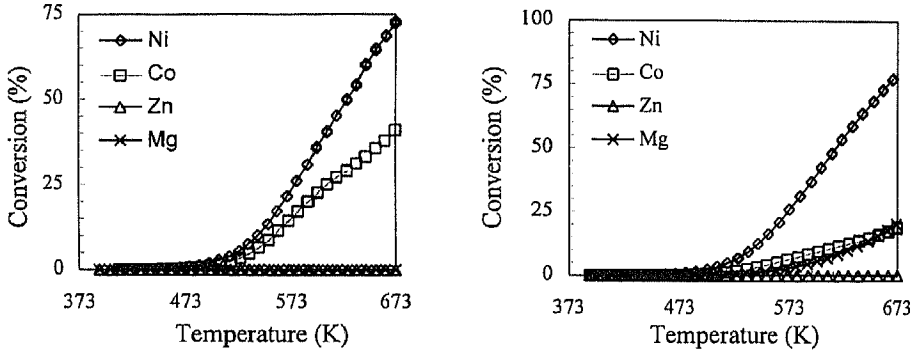

Figure 9. Performance of bare Co, Ni, Zn and Mg saponites (a) and impregnated with Mo (b)

The conversion curves of the mixed Co-Mg saponites are shown in Figure 10a. As could be expected the activity of the saponites increased with the amount of Co in the octahedral layer. The drastic increase in activity going from the Co-Mg 1:11 to the 1:1 saponite is explained by the amount of Co rising from 4 wt% to 21 wt%. Figure 10b compares the HDS activity of a 4 wt % Co impregnated Mg-saponite with that of the Co-Mg 1:11 saponite.

Hardly no difference in activity is observed with both catalysts. Clearly, the addition of Mo substantially increased the activity, the co-impregnated CoMo/Mg catalyst being slightly more active than the Mo impregnated Co-Mg saponite.

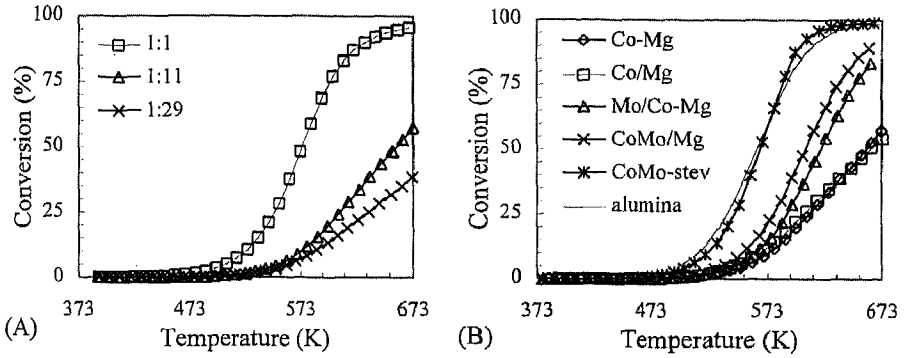

Figure 10. Performance of mixed Co-Mg saponites (A) and saponites impregnated with Co-Mo (B). Impregnated catalysts are denoted by the impregnated metal(s) / saponite support.

During the 6 hr on stream at 673 k the conversion of the saponites stabilised from conversions of 100% to the values presented here. Simultaneously the selectivity towards i-butane and C1-C3 products decreased. After oxidative regeneration and subsequent sulfiding the activity could be restored to the initial 100%. For reasons of comparison a non acidic CoMo impregnated Mg stevensite was prepared. The Mg-stevensite (no Si/Al exchange, some vacancies in the octahedral layer but no acidity) indeed showed no deactivation and the performance is comparable to that of a conventional CoMo/ γ-Al_2O_3 catalyst (13 wt % MoO_3, 4.3 wt % Co_3O_4).

4. Discussion

4.1 Distribution Co-Mg in mixed Co-Mg saponites

The ν_1(OH) and ν_2(OH) bands in the DRIFT spectra of the saponites can be attributed to the hydroxyl group of the M^{2+}-(OH) units in the octahedral sheet and the Si-OH groups present at the edges of the tetrahedral sheets, respectively [18-19]. The position of the ν_1(OH) band depends on the nature of the three coordinating octahedral ions. With two differing octahedral cations as with Co and Mg the ν_1(OH) band is expected to split in four separate bands: Mg_3-OH, Mg_2Co-OH, $MgCo_2$-OH and Co_3-OH. A random distribution of the octahedral ions with a ratio of 1:1 should result in a relative intensity of the bands of 1:2:2:1 [20]. Due to line broadening our spectra only show one broad ν_1(OH) band. In the spectrum of the Co-Mg 1:1 saponite the frequency of this band is fairly between those of the pure Mg and Co-saponite. Together with the symmetric shape of the band covering the region of the individual ν_1(OH) bands this points to a homogeneous distribution of the octahedral ions.

More detailed insight can be obtained from the EXAFS data. As can be seen from Table 1 the coordination numbers are also in accordance with a homogeneous distribution of the Mg and Co ions in the octahedral sheet. The coordination numbers $N_{Co\text{-}Co}$ and $N_{Co\text{-}Mg}$ of 0.4 and

5.8 for the Co-Mg 1:29 saponite are close to the expected values of 0.2 and 5.8, respectively. Moreover, in the Co-Mg 1:1 saponite the coordination numbers N_{Co-Co} and N_{Co-Mg} are equal showing that each Co ion is surrounded by an equal number of both Mg and Co ions. If domain segregation had taken place during synthesis the ratio N_{Co-Co}/N_{Co-Mg} would be higher than the ratio of 1.0 calculated from the stoichiometric amounts. The sum of both coordination numbers is not exact 6, but within the limits of accuracy. Alltogether, based on the DRIFT and EXAFS results, it can be concluded that in the mixed Co-Mg saponites the Co and Mg ions are uniformly distributed in the octahedral sheet.

4.2 Sulfur Resistance

To apply synthetic saponites as hydrocracking catalysts the clay lattice should be stable in an environment where rather large quantities of sulfur are present. The XRD/TEM and TPS profiles of the different saponites clearly indicate that when the octahedral layer only consists of Co, Ni or Zn the clay structure collapses upon exposure to sulfur and the bulk sulfides Co_9S_8, Ni_3S_2 and β-ZnS are formed. The Mg-saponite, however, is stable and no sulfide formation takes place. These results can be discussed in terms of the thermodynamic data of these compounds. Sulfidation of saponites with H_2S proceeds through:

$$M_3Si_4O_{10}(OH)_2 + 3\ H_2S \longrightarrow 3\ MS + 4\ SiO_2 + 4\ H_2O \qquad (1)$$

The calculated changes of Gibbs free energy of the reaction are given in Table 2. The tabulated data are those of talc minerals, a structural analogue of saponites with no Si/Al substitution in the tetrahedral layer. As less than 10 % percent of the Si is replaced by Al these data can be considered to be representative for the equivalent saponites. Data for Co talc were not available but can be expected to follow the trend of the metal oxides.

Table 2
Gibbs free energy of formation and calculated Gibbs free energy per mol metal sulfide formed for sulfidation of talcs with H_2S [21-23]

Compound	Temperature (K)	ΔG^0 (kJ/mol)	ΔG_{sulf} (kJ/mol)
$Mg_3Si_4O_{10}(OH)_2$	298	-1357	56
$Ni_3Si_4O_{10}(OH)_2$	298	-1071	-91
$Zn_3Si_4O_{10}(OH)_2$	298	-1146	-97
MgO	700	-150	33
NiO	700	-66	-70
CoO	700	-68	-59
ZnO	700	-93	-74

From Table 2 it is clear that sulfiding of a Mg saponite is thermodynamically unfavorable, whereas Ni and Zn saponites are liable to react with sulfur. The same trend is observed for the simple metal oxides including CoO. This low reactivity of Mg towards sulfur is due to the enhanced stability of Mg in an oxidic lattice compared to the other metals as indicated by the values of Gibbs free energy of formation. The enhanced stability of Co in a mixed Co-Mg saponite can thus be understood in terms of thermodynamics. Mixing Co and Mg will result in a ΔG_{sulf} intermediate between those of the pure Mg and Co saponite. Apparently, according to

our XRD observations, ΔG_{sulf} must be still postive for a Co-Mg 1:1 saponite preventing a complete collapse of the clay structure upon sulfidation at 673 K. However, the TPS pattern shows the presence of a readily sulfidable species, indicated by the low temperature consumption and production of H_2S. Most likely this species can be identified as Co atoms exposed at the edges of the clay platelets. These Co atoms are not stabilized by the clay lattice and can be considered to sulfide relatively easy. Only at temperatures above 523 K, when an increasing consumption of H_2S is observed, the more hidden Co is sulfided and extracted from the octahedral layer. It is clear, however, that at 673 K a part of Co is not sulfided and remains in the clay's octahedral layer.

4.3 HDS Activity

The HDS activity of the saponites has to be discussed both in terms of sulfur resistance and active metal sulfides. As discussed above the bare Zn, Co and Ni saponite detoriate upon sulfidation and β-ZnS, Co_9S_8, and Ni_3S_2 are formed. The latter two are known to be active in HDS, especially when these phases are highly dispersed. This explains the observed activity of the collapsed saponites. ZnS clearly is not active in HDS just as the bare Mg-saponite. The activity of the Mo impregnated Mg-saponite can entirely be ascribed to the presence of molydenum sulfide slabs. For the Zn-saponite the collapse of the clay structure causes the MoS_2 to sinter and causes subsequent loss of activity. Probably the sintering of Co_9S_8 is promoted by Mo decreasing the activity relative to the non-impregnated saponite.

It is also worthwile to compare the HDS activity of the bare Co-saponite (Fig. 9a) with the bare Co-Mg saponites (Fig 10a). This demonstrates that the specific activity of Co_9S_8 is low in comparison with the dispersed cobalt sulfide species formed after sulfiding of the mixed Co-Mg saponite. Although for the mixed Co-Mg 1:29 saponite the amount of Co is almost a factor 30 lower, the conversion is at about the same level as for the pure Co saponite. This indicates that the turnover rate for the active Co-S species is very high, indicating a high dispersion. The sulfided Co species at the edges of the clay platelets is probably very well dispersed and might even be stabilised by the clay lattice through remaining oxygen bonds. Such a species can account for the HDS activity observed. Additionally dispersed cobalt sulfide will be present supported on the saponite platelets after extraction from the clay lattice.

Remarkably, the HDS performance of the mixed Co-Mg saponite and the Co impregnated Mg support are very close. As we can fairly assume that all of the impregnated Co has been sulfided, in contrast to the mixed saponite, one might expect a larger activity of the impregnated sample. However, it seems that the lower amount of cobalt sulfide is compensated by its higher dispersion. Only when Mo is impregnated, which significantly increases the activity, the impregnated sample is slightly more active, probably as a result of a better CoMo dispersion.

As noted earlier, the saponites suffer from deactivation during HDS. This deactivation can be attributed to the acidic nature of the supports, as also indicated by the initially formed i-butane and C1-C3 products. The stevensite with no Si/Al substitution, which is therefore far less acidic, indeed does not suffer from deactivation and the performance is as good as that of a conventional CoMo/alumina catalyst. For this reason, the dispersion of the metal-sulfide phase on the stevensite, which is comparable to those on the saponite carriers, can be considered to be quite high. Further research will be directed towards the tuning of the acidic properties of the saponite and the hydrogenation properties of the metal-sulfide. This balance

plays a major role in hydrocracking, where both catalyst properties are equally important in obtaining a good activity and selectivity towards the desired products.

5.Conclusions

This study shows that saponites with only Co, Ni or Zn as octahedral ions are not stable upon exposition to H_2S and the clay structure collapses under formation of the bulk metal sulfides. Saponites with only Mg or with combinations of Mg and metals as Co or Ni incorporated in the octahedral layer are stable upon sulfidation.

Using a mixed Co-Mg saponite the Co atoms at the edges of the platelets are sulfided as part of the lattice Co. The formed Co sulfide species are highly active in the thiophene HDS and can be compared to a coventional alumina catalyst. Similar results can be obtained by impregnating bare Mg-saponites with active HDS metals such as Co/Mo.

Acknowledgements

Akzo-Nobel Chemicals B.V. is acknowledged for financial support of this research and Marianne Smolenaars and Tijmen Ros for parts of the experimental work.

References

1. J.W. Ward, Fuel Processing Technology, 35 (1993) 55.
2. J.K. Minderhoud, J.A.R. van Veen, Fuel Processing Technology, 35 (1993) 87
3. H.E . Swift in "Advanced Materials in Catalysis", eds. J.T. Burton, R.L. Garten, Academic Press, New York, (1977) 209
4. I.E. Maxwell, W.H.J. Stork ,Stud. Surf. Sci. Catal., 58 (1991) 571
5. M.L. Ocelli, R.J. Bernard, Catalysis Today, 2 (1988) 309
6. M.F. Rosa-Brussin, Catal. Rev. -Sci.Eng, 37(1) (1995) 1
7. Y. Sakata, C.H. Hamrin Jr., Ind. Chem.Prod. Res.Dev., 22 (1983) 250
8. J.T. Kloprogge, W.J.J. Welters, E. Booy, V.H.J. de Beer, R.A. van Santen, J.W. Geus, J.B.H. Jansen, App. Cat. A, 97 (1993) 77
9. R.K. Sharma, E.S. Olson, Prepr. Pap.-Am. Chem. Soc. Dive. Fuel Chem., 39 (1994) 702
10. R.J.M.J. Vogels, M.J.H.V. Kerkhoffs, J.W. Geus, Prep.Cat. VI, G. Poncelet (ed) , (1995) 1153.
11. H. Topsøe, B.S. Clausen, App. Cat., 25 (1986) 273
12. M. Vaarkamp, B.L. Mojet, M.J. Kappers, J.T. Miller, D.C. Koningsberger, J. Phys Chem., 99 (1995) 16067.
13. J.B.A. Van Zon, D.C. Koningsberger, H. Van Blik, D.E. Sayers, J. Chem. Phys., 82 (1985) 5742.
14. F.B.M. Duivenoorden, D.C. Koningsberger, Y.S. Uh, B.C. Gates, J. Am. Chem. Soc., 108 (1986) 6524.
15. J. Mustre de Leon, J.J. Rehr, S.I. Zabinsky, Phys. Rev. B, 44 (1991) 4146
16. H. Suquet, C. de la Calle, H. Pezerat, Clays and Clay Min., 23 (1975) 1
17. A. Manceau, Canadian Mineralogist, 28 (1990) 321
18. R.J.M.J. Vogels, Ph.D. Thesis, Utrecht, 1996
19. V.C. Farmer, Mineral Mag., 31 (1958) 829
20. R.W.T. Wilkins, J. Ito, Am. Mineral., 52 (1967) 1649
21. I.Barin, O. Knacke, " Thermochemical Properties of Inorg. Substances", Springer-Verlag ,1973
22. Y. Tardy, Amer. J. Sci., 279 (1979) 217
23. Y. Tardy, R.M. Garrels, Geochim. Cosmochim. Acta, 38 (1974) 1101